Available online at www.sciencedirect.com
SCIENCE DIRECT®
Acta Materialia 52 (2004) 1163–1170
Acta MATERIALIA
www.actamat-journals.com

Near-isotropic air plasma sprayed titania

R.S. Lima *, B.R. Marple

Industrial Materials Institute, National Research Council of Canada, 75 de Mortagne Blvd., Boucherville, QC J4B 6Y4, Canada

Received 13 October 2003; received in revised form 29 October 2003; accepted 5 November 2003

Abstract

A titania feedstock was air plasma sprayed on low carbon steel substrates. In-flight particle temperature, velocity and diameter were monitored in order to find a parameter set that resulted in high particle temperature and velocity. Coatings were produced using the chosen parameter set, and certain mechanical properties (Vickers microhardness, Knoop microhardness and elastic modulus) of these deposits were measured on the cross-section and in-plane (top surface). The microstructure was evaluated using image analysis (porosity) and scanning electron microscopy. Thermal spray coatings are widely known for their anisotropic character, however, in this work, the mechanical properties of the titania coatings exhibited very similar values on the cross-section and in-plane regions. The reasons why this near-isotropic character is present are suggested and discussed.

Keywords: Plasma spraying; Titania; Microindentation; Elastic behavior; Hardness

1. Introduction

In previous work [1,2], the relationships between in-flight particle characteristics, coating microstructural features and mechanical properties (microhardness and elastic modulus) of high velocity oxy-fuel (HVOF) sprayed titania coatings were investigated. The values of microhardness and elastic modulus were determined in the planes parallel and perpendicular to the deposition surface. It was observed that the microhardness and elastic modulus of these coatings exhibited near-isotropic behavior, i.e., their respective values on the cross-section and in-plane regions were very similar.

This finding was considered very interesting due to the fact that thermal spray coatings are known for exhibiting an oriented microstructure [3–8] and anisotropic behavior of mechanical properties [9–13]. It was hypothesized that the near-isotropic behavior of the HVOF-sprayed titania coatings was due to the uniform microstructural features and high densities exhibited by those coatings. It was also suggested that in order to produce these coating characteristics the use of a thermal spray feedstock having a fine particle size and a narrow particle size range was extremely important. A feedstock having these characteristics tends to have a uniform particle heating in the thermal spray jet, which is a key factor for obtaining a uniform coating microstructure [1,2]. Based on these principles, air plasma spray (APS) was applied with success for producing near-isotropic titania coatings [14]. In order to produce dense, uniform and near-isotropic coatings via APS, high particle temperatures and velocities had to be achieved.

Recently, the fundamental nature of the anisotropic behavior of thermal spray coatings has been studied using indentation techniques [10,13], modeling [9,15,16] and small-angle neutron scattering [17–19]. These studies are evidence of a growing interest in the design and engineering of thermal spray microstructures. The goal is to predict results based on a fundamental understanding of the effects of the various parameters, as opposed to using a trial-and-error approach to eventually arrive at a desired structure. It is believed that the introduction of the near-isotropic coatings discussed in this paper and earlier work will enhance the discussion and broaden the base of knowledge related to the fundamental nature of thermal spray microstructures.

* Corresponding author. Tel.:+1-450-641-5150; fax: +1-450-641-5105.
E-mail address: rogerio.lima@cnrc-nrc.gc.ca (R.S. Lima).

1359-6454/$30.00
doi:10.1016/j.actamat.2003.11.002

The objective of this work is to investigate and discuss the origins of the near-isotropic behavior of microhardness and elastic modulus in APS-sprayed titania coatings.

2. Experimental procedure

2.1. Thermal spraying and feedstock

A fused and crushed titania (TiO_2) feedstock (Flomaster 22.8(99)F4, F.J. Brodmann & Co., Harvey, LO, USA) was APS-sprayed (F4-MB, Sulzer-Metco, Westbury, NY, USA) on low carbon steel substrates (length: 7.62 cm, width: 2.54 cm, thickness: 1.27 cm) that had been grit-blasted before spraying. The nominal size range of the feedstock was from 5 to 20 μm. The spray parameters employed in this work are listed in Table 1. During the APS process a cooling system (air jets) was applied to reduce coating temperature, which was monitored by using a pyrometer. The maximum coating temperature while depositing coatings to a thickness of approximately 400 μm did not exceed 170 °C.

2.2. Particle size distribution of the feedstock

A laser diffraction particle analyzer (Beckman Coulter LS 13320, Beckman Coulter, Miami, FL, USA) was employed in order to determine the particle size distribution of the feedstock.

2.3. In-flight particle characteristics

A diagnostic tool for thermal spray particles (DPV2000, Tecnar Automation, Saint-Bruno, QC, Canada) based on optical pyrometry and time-of-flight measurements was employed to measure the distribution of particle temperature, velocity and diameter in the spray jet [20]. A total of 3000 particles were measured at the centerline of the plasma jet, where the particle flow density was the highest. The particle detector was placed at the same spray distance as used when depositing the coatings, i.e., 10 cm.

Table 1
Spray parameters used for the APS torch

Parameters	Value
Primary gas (Ar) flow (slpm)	40
Secondary gas (H_2) flow (slpm)	14.8
Current (A)	600
Voltage (V)	69.6
Power (kW)	41.8
Carrier gas (Ar) flow (slpm)	3
Powder feed rate (g/min)	20
Powder injector size (diameter) (mm)	1.8
Powder injector distance (mm)	6
Powder injector angle (°)	90
Spray distance (cm)	10

2.4. Microstructural characterization

The cross-section and in-plane (top surface) regions of the coatings were vacuum impregnated with a low viscosity epoxy and then polished to a mirror finish. The microstructures of the cross-section and in-plane regions were evaluated via scanning electron microscopy (SEM). The porosity of the coating was evaluated using image analysis on the cross-section (5 SEM pictures).

2.5. Mechanical properties

Vickers hardness, Knoop hardness and elastic modulus (E) were evaluated on the cross-section and in-plane (top surface) regions of the coatings. The elastic modulus values were determined using Knoop indentation measurements [21]. The Knoop technique employed to measure E is based on the measurement of the elastic recovery of the dimensions of the Knoop indentation impressions. The ratio of the major (a) to minor (b) diagonals of the Knoop indenter is 7.11. During unloading, the elastic recovery reduces the length of the minor diagonal of the indentation impression (b'), while the length of the major diagonal of the indentation impression (a') remains relatively unaffected. The known major to minor diagonal ratio (7.11) of the indenter is compared to that of the indentation impression. The extent of recovery depends on the hardness-to-modulus (H/E) ratio of the material being indented. The formula for determining the elastic modulus (E, in Pa) is [21]:

$$E = \frac{(-\alpha H)}{((b'/a') - (b/a))}, \tag{1}$$

where α is a constant (0.45), H is the Knoop hardness (in Pa), a' and b' are the lengths of the major and minor diagonals of the Knoop indentation impression, and b/a is 1/7.11. An important point should be noted. For the cross-section, the indentations were applied near the centerline of the coating thickness. Two series of Knoop indentations were performed on the cross-section: (i) the major diagonal of the Knoop indenter positioned perpendicular to the substrate surface $E_{cs\perp}$ (20 indentations) and (ii) the major diagonal of the Knoop indenter positioned parallel to the substrate surface $E_{cs||}$ (10 indentations). For the in-plane direction E_{ip}, the indentations (Knoop and Vickers) were randomly positioned over the coating surface (20 indentations).

A load of 1000 g and an indentation time of 15 s were applied for the Knoop hardness and E measurements. For the Vickers hardness, the indentation load and time were 300 g and 15 s, respectively.

3. Results and discussion

3.1. In-flight particle characteristics

Fig. 1 shows the plot of particle temperature versus particle diameter distribution in the plasma jet. Almost all particles have temperatures (at least superficially) higher than the melting point of the titania, which is 1855 °C [22]. The average particle temperature is 2702 ± 217 °C, and the coefficient of variation (CV) is 8%, i.e., the relative dispersion of particle temperature is low. This means that the sprayed particles were uniformly heated in the plasma jet. As the temperatures of the particles were measured via pyrometry, it is important to point out that errors related to calibration may be present. This is a typical characteristic of pyrometric measurements, and therefore, the real particle temperature values may be higher or lower than those measured.

The distribution of particle velocity in the spray jet is plotted in Fig. 2. The average particle velocity is 266 ± 63 m/s. This is a high velocity for APS-sprayed particles. Velocity measurements of APS-sprayed ceramic particles at a spray distance of 10 cm (the same distance employed in this work) show that the typical average velocity values are in a range of 120–180 m/s [23]. For the present case, not one of the 3000 measured particles exhibited velocities lower than 125 m/s and some of them attained velocities close to 500 m/s (Fig. 2). As previously mentioned in the Introduction section, dense and uniform coatings seem to be of high importance if near-isotropic coatings are to be achieved [1,2]. Consequently, the high particle velocities and low CV of particle temperature attained in this work should provide conditions for producing coatings having a near-isotropic behavior.

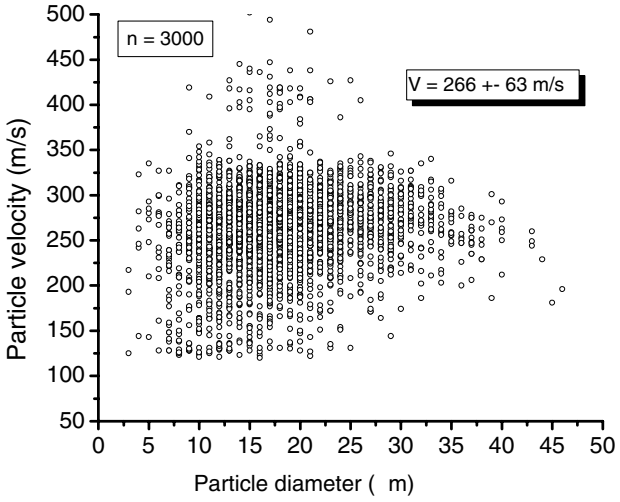

Fig. 2. Particle velocity versus particle diameter distribution in the plasma jet.

According to Figs. 1 and 2, the particle size range of the particles in the spray jet varied from 5 to 50 μm. The particle size distribution (in volume) of the titania feedstock determined using laser scattering is shown in Fig. 3. The results of d_{10}, d_{50} and d_{90} were 8, 19 and 46 μm, respectively. Consequently the particle size distribution registered during the in-flight particle analysis using pyrometry (Figs. 1 and 2) is a fair representation of the real particle size range of the feedstock. These results show that the diagnostics equipment was well calibrated.

Despite exhibiting a true particle size range larger than the nominal one, this feedstock still has relatively fine particles and a narrow particle size distribution. These characteristics certainly contributed to producing the low particle temperature distribution and high particle velocity in the spray jet.

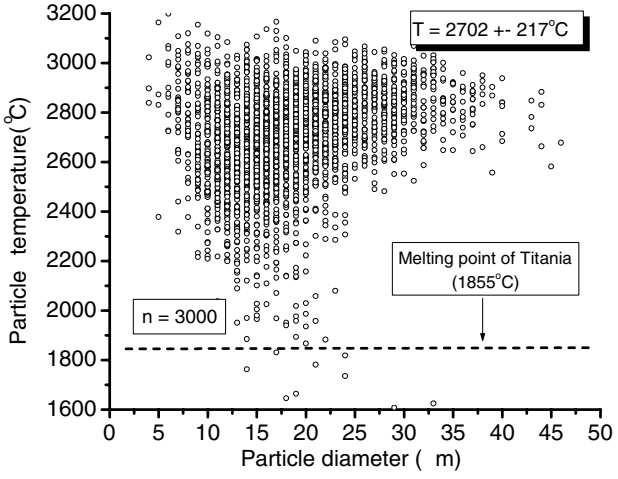

Fig. 1. Particle temperature versus particle diameter distribution in the plasma jet.

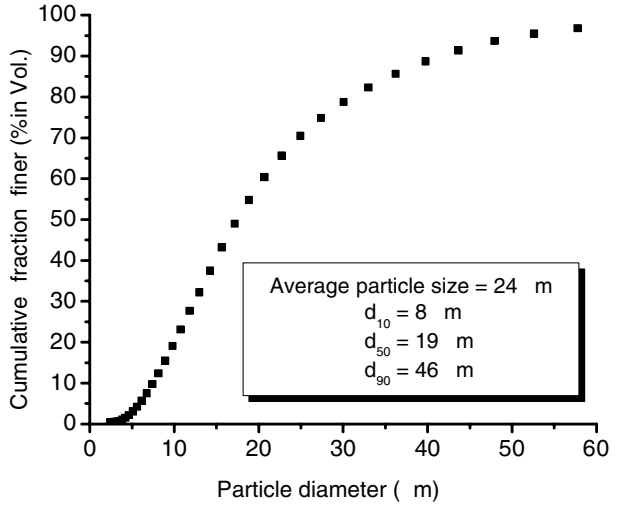

Fig. 3. Particle size distribution of the titania feedstock determined by laser scattering.

3.2. Microstructure

The SEM pictures of the cross-section and in-plane regions of the titania coatings are shown in Figs. 4 and 5. The coating is dense; the porosity measured by image analysis was <1%. The microstructure is uniform but the traditional pancake-shaped splats or lamellas of thermal spray coatings are not readily observed (Fig. 4). However, with careful inspection it is possible to distinguish features related to a layered structure, like the parallel darkish bands generated during successive torch passes indicated by arrows in Fig. 4. Nonetheless, due to the extensive series of vertical intra-splat microcracks and the high density of the coating, the layered structure does not seem to be a dominant characteristic of the microstructure (Fig. 4). In fact, the in-plane region of the coating (Fig. 5) resembles a bulk ceramic microstructure.

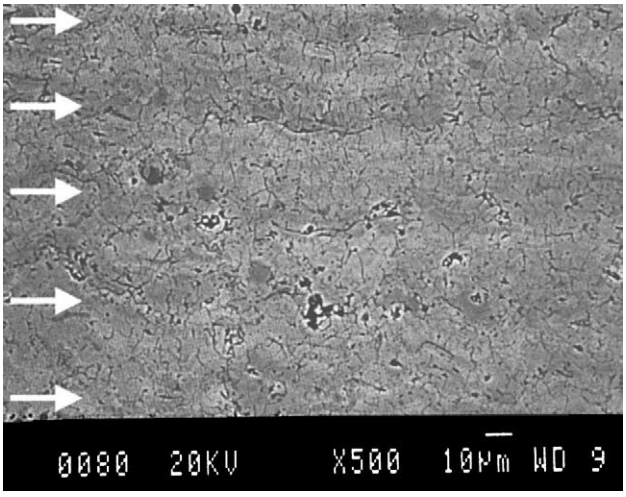

Fig. 4. SEM picture of the cross-section region of the APS-sprayed titania coating.

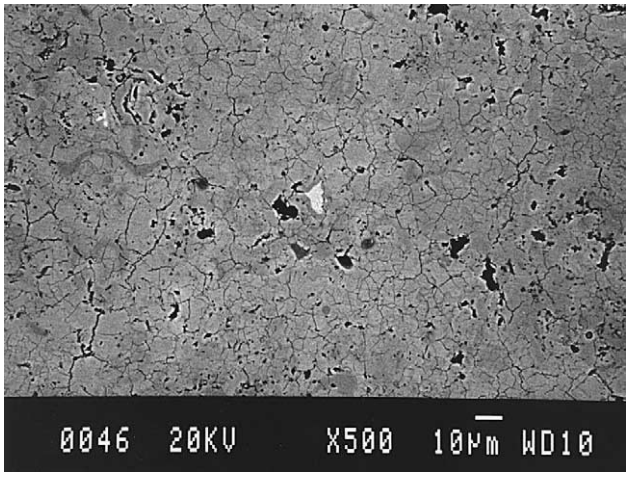

Fig. 5. SEM picture of the in-plane region of the APS-sprayed titania coating.

It is important to point out that the average particle size of the feedstock was 24 μm (Fig. 3). A fully or partially molten feedstock particle would spread during impact with the substrate surface (or previously deposited layers) and it is naturally assumed that the average diameter of the pancake-shaped splats would tend to be larger than the average particle size (24 μm) of the original feedstock. Nonetheless, by taking a close look at the microstructures of Figs. 4 and 5 and their respective scale bars it is observed that the majority of the intervals between two adjacent cracks have a length equal to or smaller than 10 μm. This experimental observation shows that the formation of the vertical intra-splat crack network in the coating microstructure was very significant and, due to this feature, a proper identification (visualization) of the lamellar structure is not possible. In other words, it may be stated that the extensive vertical cracking that occurred for this coating masked its lamellar structure.

The crack formation in APS-sprayed zirconia coatings was investigated in earlier research [20]. It was concluded in that work that the particle temperature had an important effect on the formation of a vertical crack network, i.e., higher particle temperatures yield higher levels of vertical cracking. This conclusion seems to agree very well with other work [24], where ceramic splats exhibited vertical cracks that were caused by quenching (during impact), lack of plasticity and subsequent stress relaxation. Higher particle temperatures should increase the intensity of quenching and cracking. In the present study, it is necessary to remember that the majority of the sprayed particles exhibited superficial temperatures much higher than the melting point of titania (Fig. 1). Therefore the extensive vertical crack network observed in this work agrees with the experimental observations of the other researchers [20,24]. This extensive crack network and the apparent absence of the lamellar structure seem to be important keys for producing coatings with similar mechanical properties (elastic modulus and hardness) values on the cross-section and in-plane regions, as will be discussed in the following sections.

3.3. Mechanical properties

The values of hardness and elastic modulus and their respective ratios on the cross-section and in-plane regions are listed in Table 2. A schematic of the indentation positions in relation to the thermal spray microstructure is shown in Fig. 6. It can be observed that depending on the orientation of the major diagonal of the Knoop indenter two distinctive morphological zones in the cross-section (parallel and perpendicular to

Table 2
Coating properties and property value ratio for the APS-sprayed titania coating

Mechanical property	Cross-section (CS)	In-plane (IP)	CS/IP ratio
HV (300 g)	804 ± 50	835 ± 56	0.96
HK (1000 g)	729 22 (major diagonal $\perp$ substrate) 615 ± 28 (major diagonal || substrate)	722 ± 14	1.01 (major diagonal $\perp$ substrate) 0.85 (major diagonal || substrate) $HK_{cs\|\|}/HK_{cs\perp}$ *ratio*: 0.85
E (GPa)	117 ± 22 (major diagonal $\perp$ substrate) 135 ± 36 (major diagonal || substrate)	112 ± 10	1.04 (major diagonal $\perp$ substrate) 1.21 (major diagonal || substrate) $E_{cs\|\|}/E_{cs\perp}$ *ratio*: 1.15

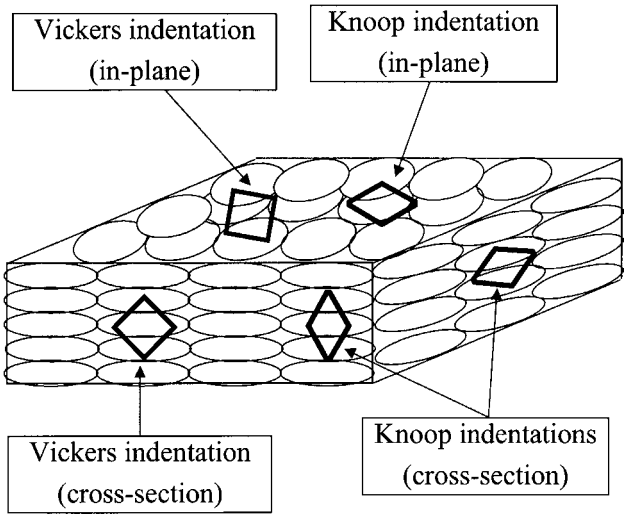

Fig. 6. Schematic of a thermal spray microstructure and the Knoop and Vickers indentation zones in a thermal spray coating.

the substrate surface) and one zone in the in-plane regions can be probed. Because of the differences in microstructure, it is expected that the mechanical interactions between an indenter and the coating will be different for these zones, producing distinctive values of mechanical properties, as normally observed in thermal spray coatings [9–13]. Concerning the orientation of the Vickers indentations, two distinctive morphological zones are probed, one in the cross-section and one in the in-plane regions (Fig. 6).

From Table 2, it is observed that the elastic behavior of the coating is similar in the cross-section and in-plane directions; i.e., the ratio between E values in the three zones ($E_{cs||}/E_{ip}$, $E_{cs\perp}/E_{ip}$, $E_{cs||}/E_{cs\perp}$) probed is close to unity. The same characteristic, i.e., ratio close to unity, is also observed for the hardness values (Table 2). Some E values determined via Knoop indentation in the cross-section and in-plane regions of thermal spray coatings (using the same load and indentation positioning as those employed in this study) are reported in the literature [10–12]. According to reference [10] the $E_{cs\perp}/E_{ip}$ ratio varies from 1.5 to 1.9. The same ratio for reference [11] varies from 1.01 to 3.33, whereas for reference [12] it is 1.45. Therefore, typical thermal spray coatings exhibit an anisotropic behavior when in-plane and cross-section properties are compared. This characteristic contrasts with the results obtained for the coatings produced in this study where a near-isotropic behavior was observed. As all the ratios found for this titania coating are close to unity, these data from the literature support the proposed claim that this titania thermal spray coating is exhibiting near-isotropic behavior.

As previously observed [1,2], high density and microstructural uniformity are very important if the objective is producing near-isotropic thermal spray coatings. In the work of Allen et al. [19], APS-sprayed zirconia coatings were annealed at temperatures up to 1400 °C during 1 h. The elastic modulus values (cross-section and in-plane) of the as-sprayed and annealed coatings were determined using Hertzian indentation, and the voids of the coatings (cracks and pores) were evaluated via SEM, density determination, and multiple small-angle neutron scattering (MSANS). It was reported that the maximum reduction of porosity due to the annealing was ~15%, and the maximum reduction in surface area was ~60%. It was observed that the as-sprayed zirconia coatings exhibited a high degree of anisotropy ($E_{cs}/E_{ip} \sim 1.55$); however, during annealing, the degree of anisotropy started to decrease, reaching a value of (E_{cs}/E_{ip}) ~1.1 when the porosity and the surface area were reduced to their respective lowest values [19]. Wallace and Ilavsky [13] produced APS zirconia coatings with different porosity levels by changing the spray distance (the greater the spray distance, the higher the porosity). The elastic modulus values of these coatings were measured on the cross-section and in-plane regions. It was found that the degree of anisotropy was lower for the denser coatings, i.e., the anisotropic behavior became more pronounced at higher coating porosity levels (produced at long spray distances).

It should be remembered that the total porosity (surface area) of thermal spray coatings is formed from different porosity elements, such as globular pores, inter-splat pores and intra-splat cracks [3–10,15–19]. Modeling results show that these various types of porosity

have different roles and weights in the overall mechanical behavior of a coating [9,15,16]. Allen et al. [19] observed that the healing behavior of these different porosity elements during annealing was distinct for each group, i.e., they sinter or transform (coarsen) in different modes and at different rates. Nonetheless, these researchers [13,19] observed that when the overall surface area began to decrease, the anisotropic character of the mechanical properties tended to be reduced (even if the porosity elements were healing differently [19]). These observations tend to support the assumption that producing dense coatings is important for obtaining near-isotropic behavior.

3.4. Origin of the near-isotropic behavior

The reason for the anisotropic behavior of ceramic thermal spray coatings has been well explained by Leigh et al. [10] and Wallace and Ilavsky [13]. In order to understand this phenomenon, it is necessary to recall that the surface area of the different porosity elements reduces the elastic modulus and hardness values of ceramic materials [25,26]. Measurements of microhardness and/or elastic modulus of thermal spray coatings have shown higher values on the cross-section than on the in-plane regions [10–13,27]. This phenomenon can be explained based on the shapes and orientations of pores and cracks. Inter-splat pores and intra-splat cracks may be considered as ellipses having different aspect ratios (ratio of the major axis over the minor axis) and regarded as pores parallel and perpendicular to the substrate surface, respectively. It is known that each pancake-shaped splat is horizontally oriented with dimensions of approximately 1 μm thick and 50 μm in diameter [28]. Due to this geometrical factor, the surface area provided by horizontal inter-splat pores will tend to be higher than that provided by the vertical intra-splat cracks [10,13,19].

Therefore the higher surface area provided by the horizontal inter-splat pores is responsible for the decrease in microhardness and elastic modulus values when measured in the plane parallel to the substrate surface (in-plane region). On the other hand, the lower surface area provided by the vertical intra-splat cracks results in higher microhardness and elastic modulus values when measured on the cross-section. Therefore, based on crack-pore orientation and surface area it is possible to understand why the mechanical properties of thermal spray coatings tend to be anisotropic.

Explaining the near-isotropic behavior of thermal spray coatings is more complicated. Modeling may be an important tool in order to better understand and quantify the origin and causes of the near-isotropic behavior. The elastic modulus properties of thermal spray coatings have been modeled by Kroupa et al. [15,16] as a function of globular pores, inter-splat pores and intra-splat cracks. According to the model, the material comprising the splats is isotropic and homogeneous, exhibiting an elastic modulus E_0 and a Poisson's ratio v_0. Within the thermal spray coating there are randomly distributed, approximately spherical (globular) pores of radii R_i. The overall coating porosity, p, is given by:

$$P = (1/V)\sum_{i=1}^{N}(4/3)\pi R_i^3, \tag{2}$$

where V is the representative volume element (cracks do not contribute to porosity p). The imperfect bonding between splats along the interfaces (boundaries) is represented by a family of approximately circular and randomly distributed microcracks of radii r_3 parallel to the substrate surface. Their effect is given in terms of a scalar crack density ρ_3:

$$\rho_3 = (1/V)\sum_{i=1}^{n} r_{3i}^3. \tag{3}$$

Vertically oriented cracking is represented by a family of approximately circular and randomly distributed microcracks of radii r_1 perpendicular to the substrate surface. Their effect is given in terms of a scalar crack density ρ_1:

$$\rho_1 = (1/V)\sum_{i=1}^{n} r_{1i}^3. \tag{4}$$

According to this model [15,16] the resulting elastic modulus (E) values are given by two equations. For E values parallel to the substrate surface (equivalent to E measurements via Knoop indentation with the major diagonal perpendicular to the substrate surface):

$$E_1 = E_0/\{1 + (p/1-p)[3(1-v_0)(9+5v_0)/2(7-5v_0)] + (\rho_1/1-p)[8(1-v_0^2)(1-3v_0/8)/3(1-v_0/2)]\}. \tag{5}$$

For E values perpendicular to the substrate surface (equivalent to E measurements via Knoop indentation with the major diagonal parallel to the substrate surface):

$$E_3 = E_0/\{1 + (p/1-p)[3(1-v_0)(9+5v_0)/2(7-5v_0)] + (\rho_3/1-p)[16(1-v_0^2)/3]\}. \tag{6}$$

In an attempt to gain insight into the behavior of the titania coating being evaluated in the present study, values of E_0 (283 GPa) and v_0 (0.28) for rutile (the major phase of the coating [14]) were taken from the literature [22] and substituted into Eqs. (5) and (6) proposed by Kroupa et al. [15,16]. As the porosity of the coating (determined by image analysis) was less than 1%, the plots of the elastic modulus values versus scalar crack density were carried out for porosity values of 0% and 1%, in order to give a fair representation of the overall

coating behavior. These plots are represented in Figs. 7 and 8.

It is observed that the coatings tend to have near isotropic values of elastic modulus when the scalar crack density perpendicular to the substrate surface is approximately two times the scalar crack density parallel to the substrate surface. In other words, when the effect of the surface area created by the vertical intra-splat cracks is large enough to balance the effect of the surface area created by the horizontal inter-splat pores, the elastic behavior of a ceramic thermal spray coating will tend to be near-isotropic.

In order to achieve this type of microstructure, the cross-section of the thermal spray coating would have to exhibit a significant vertical intra-splat crack network, in order to balance the surface area of the horizontal inter-splat pores. A dense coating also would be important because it would reduce the surface area of the horizontal inter-splat pores. As previously discussed, the titania coating produced in this study was very dense (porosity less than 1%) and, by looking at the microstructures of Figs. 4 and 5, it is noticed that a significant vertical cracking was produced in the coating microstructure. Consequently, these experimental observations and the near-isotropic behavior observed for this APS-sprayed titania coating tend to agree with the modeling proposed by Kroupa et al. [15,16].

The microstructure of thermal spray coatings is quite complex. Quantifying with precision the surface areas or volumes of cracks and pores requires very complex techniques such as neutron scattering [13,17–19]; which is not readily available in the majority of the research centers and universities. It will be necessary to employ this type of technique in order to determine the surface areas of cracks and pores and better understand the near-isotropic behavior of the coatings produced in this study. This is the next objective of the authors for the continuation of this work.

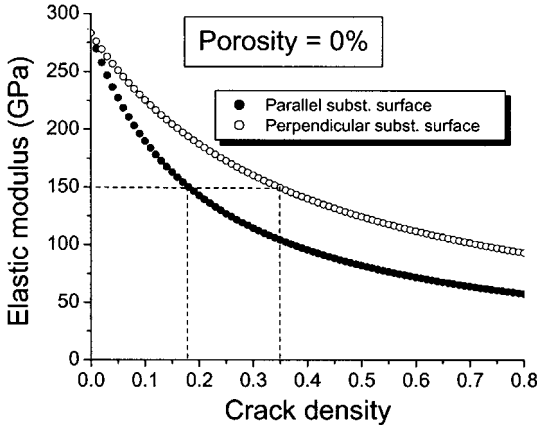

Fig. 7. Modeling of the elastic modulus parallel and perpendicular to the substrate surface for a titania thermal spray coating versus the scalar crack density (coating porosity 0%).

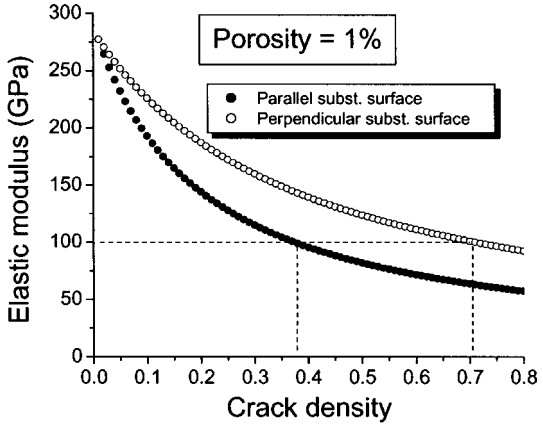

Fig. 8. Modeling of the elastic modulus parallel and perpendicular to the substrate surface for a titania thermal spray coating versus the scalar crack density (coating porosity 1%).

4. Conclusions

1. Titania coatings produced by APS spraying exhibited a near-isotropic behavior of elastic modulus and hardness with respect to the cross-section and in-plane regions of the coating. This is an interesting and somewhat novel finding since thermal spray coatings are generally considered as being inherently anisotropic.
2. The traditional lamellar structure of thermal spray coatings was apparently absent for the APS-sprayed titania. It was experimentally observed that the titania coating had a very dense microstructure and an extensive vertical intra-splat crack network that probably inhibited the manifestation of a noticeable lamellar structure. This seems to be a key factor for producing near-isotropic coatings.
3. The explanation for the origin of the near-isotropic behavior can be hypothesized using the results of modeling analysis. The elastic modulus of the cross-section and in-plane regions will tend to exhibit a near-isotropic behavior when the surface area of the vertical intra-splat cracks is approximately twice the surface area of the horizontal inter-splat pores.
4. It is thought that the apparent absence of a lamellar structure was due to the effect of the increased surface area perpendicular to the substrate surface generated by the extensive vertical cracking, which balanced the low surface area effect (high coating density) generated by the horizontal inter-splat pores parallel to the substrate surface. It is believed that this vertical/horizontal surface area balance caused the near-isotropic behavior. The experimental observations seem to support this hypothesis.
5. The extensive vertical intra-splat crack network observed in the APS-sprayed titania was probably

caused by high stresses generated during quenching of the sprayed particles from high temperature.

6. Almost all particles in the spray jet exhibited superficial temperatures well above the melting point of titania, and low particle temperature dispersion (CV = 8%). Therefore, the feedstock particles were uniformly heated during spraying, a factor that, combined with the high average particle velocity (for an APS system), probably favored the production of a dense and uniform coating.

Acknowledgements

The authors thank P. Marcoux for revision of this work, S. Bélanger for APS spraying, M. Lamontagne for the DPV2000 measurements, É. Poirier for metallography and M. Thibodeau for his assistance with X-ray diffraction analysis, scanning electron microscopy and laser diffraction particle analysis.

References

[1] Lima RS, Marple BR. J Therm Spray Technol 2003;12(2):240.
[2] Lima RS, Marple BR. J Therm Spray Technol 2003;12(3):360.
[3] McPherson R. Surf Coat Technol 1989;39/40:173.
[4] McPherson R, Shaffer BV. Thin Solid Films 1982;97:201.
[5] McPherson R. Thin Solid Films 1981;83:297.
[6] McPherson R. Thin Solid Films 1984;112:89.
[7] Leigh SH, Berndt CC. J Am Ceram Soc 1999;82(1):17.
[8] Li CJ, Ohmori A. J Therm Spray Technol 2002;11(3):365.
[9] Nakamura T, Qian G, Berndt CC. J Am Ceram Soc 2000;83(3):578.
[10] Leigh SH, Lin CK, Berndt CC. J Am Ceram Soc 1997;80(8):2093.
[11] Kim HJ, Kweon YG. Thin Solid Films 1999;342:201.
[12] Li J, Ding C. Surf Coat Technol 2001;135:229.
[13] Wallace JS, Ilavsky J. J Therm Spray Technol 1998;7(4):521.
[14] Lima RS, Marple BR. Comparative study of HVOF and APS titania coatings. In: Dahotre N, Iroh JO, Herring D, Midea S, Kopech H, editors. Paper #ISEC-00072, pdf format in the Proceedings from the 1st International Surface Engineering Congress and the 13th IFHTSE Congress. Materials Park (OH, USA): ASM International; 2003. p. 515–9.
[15] Kroupa F, Dubsky J. Scr Mater 1999;40(11):1249.
[16] Kroupa F, Kachanov M. Effect of microcracks and pores on the elastic properties of plasma sprayed materials. In: Carstensen JV, Leffers T, Lorentzen T, Petersen OB, Sorensen BF, Winther G, editors. Modelling of structure and mechanics of materials from microscale to products. Roskilde, Denmark: Riso National Laboratory; 1998. p. 325.
[17] Ilavsky J, Long GG, Allen AJ, Leblanc L, Prystay M, Moreau C. J Therm Spray Technol 1999;8(3):414.
[18] Ilavsky J, Allen AJ, Long GG, Krueger S, Berndt CC, Herman H. J Am Ceram Soc 1997;80(3):733.
[19] Allen AJ, Ilavsky J, Long GG, Wallace JS, Berndt CC, Herman H. Acta Mater 2001;49:1661.
[20] Prystay M, Gougeon P, Moreau C. J Therm Spray Technol 2001;10(1):67.
[21] Marshall DB, Noma T, Evans AG. J Am Ceram Soc 1982;65(10):C–175.
[22] Miyayama M, Koumoto K, Yanagida H. Engineering properties of single oxides. In: Schneider SJ, editor. Engineered materials handbook. Ceramic and glasses, vol. 4. Materials Park, OH, USA: ASM International; 1991. p. 748.
[23] Pawlowski L. The science and engineering of thermal spray coatings. Chichester: Wiley; 1995.
[24] Kuroda S, Clyne WT. Thin Solid Films 1991;200:49.
[25] Yang JF, Ohji T, Kanzaki S, Diaz A, Hapshire S. J Am Ceram Soc 2002;85(6):1512.
[26] Camerucci MA, Urretavizcaya G, Cavalieri AL. J Eur Ceram Soc 2001;21:1195.
[27] Lima RS, Kucuk A, Berndt CC. Surf Coat Technol 2001;135:166.
[28] Kucuk A, Lima RS, Berndt CC. J Am Ceram Soc 2001;84(4):685.